Available online at www.sciencedirect.com
ScienceDirect
European Journal of Pharmaceutics and Biopharmaceutics 69 (2008) 1057–1066
European Journal of Pharmaceutics and Biopharmaceutics
www.elsevier.com/locate/ejpb

Research paper

Nebulization of nanoparticulate amorphous or crystalline tacrolimus – Single-dose pharmacokinetics study in mice

Prapasri Sinswat [a], Kirk A. Overhoff [a], Jason T. McConville [a], Keith P. Johnston [b,*], Robert O. Williams III [a,*]

[a] The University of Texas at Austin, TX, USA
[b] Department of Chemical Engineering, The University of Texas at Austin, TX, USA

Received 12 March 2007; accepted in revised form 29 January 2008
Available online 16 February 2008

Abstract

Developing a pulmonary composition of tacrolimus (TAC) provides direct access to the graft in lung transplant offering the possibility of high drug levels. The objective of this study was to investigate the physicochemical and pharmacokinetic characteristics of the nanostructured aggregates containing amorphous or crystalline nanoparticles of TAC produced by ultra-rapid freezing (URF). TAC and lactose (1:1 ratio; URF-TAC:LAC) and TAC alone (URF-TAC) were investigated for pulmonary delivery and compared to unprocessed TAC. X-ray diffraction (XRD) results indicated that URF-TAC was crystalline, whereas URF-TAC:LAC was amorphous. *In vitro* results revealed the superior physiochemical characteristics of both URF formulations compared to unprocessed TAC. The surface area of URF processed TAC was higher (25–29 m^2/g) than that of the unprocessed TAC (0.53 m^2/g) and subsequently enhanced dissolution rates. In addition, URF-TAC:LAC displayed the ability to supersaturate in the dissolution media to about 11 times the crystalline equilibrium solubility. Similar aerodynamic particle sizes of 2–3 μm, and fine particle fraction between 70% and 75% were found in both formulations. The local and systemic pharmacokinetic studies in mice showed similar $AUC_{(0-24)}$, higher C_{max}, and lower T_{max} for the URF-TAC:LAC compared to the URF-TAC. Nanostructured aggregates containing amorphous or crystalline nanoparticles of TAC were demonstrated to be effectively delivered via nebulization, with similar *in vitro* and *in vivo* performances.

Keywords: Tacrolimus (TAC); Ultra-rapid freezing (URF); Nanoparticles; Amorphous; Crystalline; Pulmonary delivery

1. Introduction

Tacrolimus (TAC) is a widely used immunosuppressive agent isolated from *Streptomyces tsukubaensis*. It has proven to be a potent immunosuppressant in transplantation medicine for treatment of organ rejection and different immunological diseases such as pulmonary fibrosis and bronchiolar asthma [1–3]. TAC was first introduced as rescue therapy when cyclosporin A (CsA) therapy failed to prevent graft rejection [4]. It has a mechanism of action similar to that of CsA, but its immunosuppressive activity is 10 to 100 times more potent than CsA [5]. TAC is currently available in both an intravenous and an oral dosage form (commercially known as Prograf®). However, these current available dosage forms of the drug are poorly tolerated and provide a variable and/or low bioavailability [6]. The oral formulations of TAC present a considerable challenge as the drugs are practically insoluble in water and extensively metabolized from both CYP3A4 metabolism and p-glycoprotein efflux transport within the intestinal epithelium [7]. The oral bioavailability of TAC varies from 4% to 93% [8]. Inefficient or erratic drug absorption is primarily the result of incomplete absorption from the

* Corresponding authors. Department of Chemical Engineering, The University of Texas at Austin, Austin, TX 78712, USA. Tel.: +1 512 471 4617; fax: +1 512 475 7824 (K.P. Johnston); Division of Pharmaceutics, College of Pharmacy, The University of Texas at Austin, Austin, TX 78712-1074, USA. Tel.: +1 512 471 4681; fax: +1 512 471 7474 (R.O. Williams III).
E-mail addresses: kpj@che.utexas.edu (K.P. Johnston), williro@mail.utexas.edu (R.O. Williams III).

0939-6411/$ - see front matter © 2008 Elsevier B.V. All rights reserved.
doi:10.1016/j.ejpb.2008.01.037

gastrointestinal tract and first-pass metabolism, which is subject to considerable inter-individual variation [8].

This study focused on investigating a first pulmonary drug delivery system based on nanoparticles of TAC in order to overcome the above-mentioned problems to improve bioavailability. The appealing aspects of inhaled drug nanoparticles include rapid dissolution of nanoparticles in the lung and the avoidance of hepatic first-pass metabolism (which is especially useful for a drug that undergoes extensive metabolism in liver) [9–11]. Additionally, inhaled nanoparticles can increase local drug concentrations in the lung for potential therapeutic use in lung transplantation and pulmonary diseases. The treatment of lung transplant recipients is often limited due to poor penetration of drug into the lung following oral or intravenous administration [12]. Aerosolized drug will have direct access to the graft in lung transplant offering the possibility of much higher drug levels [13,14]. However, a major disadvantage of pulmonary delivery for drugs like TAC is limitations in the levels and types of excipients that are considered safe to use in pulmonary formulations. Lactose is the most commonly used as the excipient for pulmonary delivery since it is approved by the Food and Drug Administration (FDA) as excipient for inhalation purposes [15]. This is due to their non-toxic, its broad availability, relatively low price and readily degradable properties after administration. In addition, lactose can inhibit crystallization of drug in amorphous phase and prevent nanoparticle aggregation upon lyophilization leading to a high dissolution of drug product [16].

Although many surfactants or polymers such as cyclodextrins, poloxamers, polyethylene glycols (PEG) and glycerol have been studied in pulmonary formulations to aid drug solubilization in many research studies [17–19], these excipients have not been approved yet for commercial use by the FDA because of potential toxicity in the lung. Several clinical studies have demonstrated effective pulmonary delivery of CsA solutions in ethanol or propylene glycol prior to aerosolization in lung transplantation models [20–22]. However, the solvents that have produced the results have shown to be unsatisfactory due to the irritating properties of the solventsation to the airways. In addition, the use of high levels of ethanol or propylene glycol in formulations intended for pulmonary delivery has yet to be widely studied in humans. Recently, liposome technology has been investigated as a non-irritating alternative for pulmonary delivery of CsA, but the formulation had low drug loading and thus requires a lengthy nebulization period [23].

In this present study, pulmonary formulations containing TAC manufactured by ultra-rapid freezing (URF), without the inclusion of surfactants or polymeric excipients, were investigated. URF technology is a continuous, scalable cryogenic process produces nanostructured aggregates with high surface area resulting in high enhanced drug dissolution rates. Previously, spray freezing into liquid (SFL) was reported [24–29]. The rapid freezing rates achieved with the SFL process led to the production of amorphous nanostructured aggregates composed of primary particles, ranging from 100 to 200 nm, with high surface areas, high wettability and significantly enhanced dissolution rates. The URF process yields particles with similar properties as those produced by SFL. In URF a solution of the active and excipient in a suitable organic solvent or aqueous co-solvent is applied to the surface of a cryogenic solid substrate. The solution is frozen very quickly in 50 ms to 1 s, onto the surface of cryogenic solid substrate in a continuous manner [30,31]. URF powders exhibit desirable properties for enhancing bioavailability such as high surface area, increased drug dissolution rates, and amorphous character.

The objective of this study was to demonstrate that nanostructured aggregates composed of amorphous or crystalline nanoparticles of TAC produced by the URF process are suitable for pulmonary delivery by nebulization, resulting in high lung and blood concentrations. The hypothesis is that high surface area and rapid dissolution rate obtained from nanostructured aggregates of TAC promote high systemic drug absorption via the lung, while still maintaining a desirable pulmonary residence time for potential local therapy.

Relevant physicochemical properties (e.g. surface area, dissolution, morphology and crystallinity) of TAC nanostructured aggregates were characterized in order to understand how they influence drug deposition and absorption following single-dose nebulization. The aerosol performance and deposition of TAC were determined using an 8-stage cascade impactor after aerosolization via an Aeroneb®. *In vivo* studies were conducted in mice by dispersing the URF formulations in deionized water and nebulizing the dispersed URF formulations using a specially designed nose-only dosing apparatus. Determination of tissue and serum concentrations was performed to characterize pharmacokinetic parameters for TAC.

2. Materials and methods

2.1. Materials

TAC was kindly provided by The Dow Chemical Company (Midland, MI). Anhydrous lactose, magnesium chloride hexahydrate, sodium chloride, potassium chloride, sodium phosphate dibasic anhydrous, sodium sulfate anhydrous, calcium chloride dihydrate, sodium acetate trihydrate, sodium bicarbonate and sodium citrate dihydrate were of analytical grade and purchased from Spectrum Chemicals (Gardena, CA). Dipalmitoylphosphatidylcholine (DPPC) was purchased from Sigma–Aldrich Chemicals (Milwaukee, WI). High performance liquid chromatography (HPLC) grade acetonitrile (ACN) was purchased from EM Industries, Inc. (Gibbstown, NJ). Liquid nitrogen was obtained from Boc Gases (Murray Hill, NJ). Deionized water was prepared by a Milli-Q purification system from Millipore (Molsheim, France).

2.2. Preparation of URF formulations

TAC formulations were processed using URF. A schematic diagram of the URF process is illustrated in Fig. 1. Two URF formulations considered for pulmonary delivery were TAC:lactose in a 1:1 ratio (URF-TAC:LAC) and TAC alone (URF-TAC). The compositions were prepared by dissolving TAC and hydrophilic excipient (if any) at a 1:1 ratio and 0.75% solids in a 60/40 mixture of acetonitrile and water. The solution of drug was applied to the surface of solid substrate made from metal, which is cooled using liquid nitrogen as cryogenic substrate maintained at −50 °C. The frozen compositions were then collected and the solvent was removed by lyophilization using VirTis Advantage Tray Lyophilizer (VirTis Company Inc., Gardiner, NY). The dried powders were stored at room temperature under vacuum.

2.3. In vitro characterization of powders for pulmonary

2.3.1. X-ray powder diffraction (XRD)

The XRD patterns of the powders were analyzed using a Philips 1710 X-ray diffractometer with a copper target and nickel filter (Philips Electronic Instruments, Inc., Mahwah, NJ). Each sample was measured from 5 to 45 2θ degrees using a step size of 0.05 2θ degrees and a dwell time of 1 s.

2.3.2. BET specific surface area analysis

Specific surface area was measured using the gas adsorption technique with nitrogen as the adsorbate gas via a Nova 2000 v.6.11 instrument (Quantachrome Instruments, Boynton Beach, FL). A known weight of powder was added to a 12 mm Quantachrome bulb sample cell. Samples were degassed by applying vacuum at room temperature for a minimum of 3 h prior to analysis. Three samples of each formulation were analyzed. The data recorded were then analyzed according to BET theory using NOVA Enhanced Data Reduction Software v.2.13. Specific surface area was determined by applying the BET model to the equilibrium isotherm within pressures of 0.05–0.30 psia. Six experimental points (BET multipoint) were used for calculation.

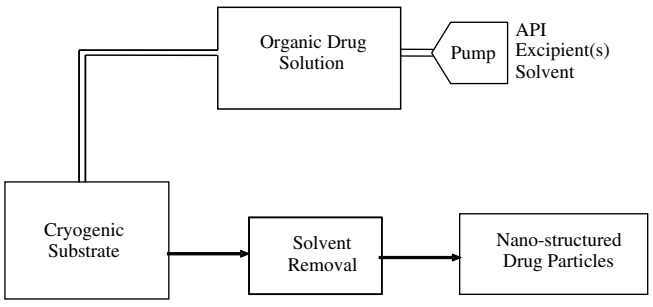

Fig. 1. Schematic representation of URF technology.

2.3.3. Scanning electron microscopy (SEM)

A Hitachi S-4500 field emission scanning electron microscope (Hitachi High-Technologies Corp., Tokyo, Japan) was used to obtain SEM micrographs of the powder samples. Samples were mounted on conductive tape and sputter coated using a model K575 sputter coater (Emitech Products, Inc., Houston, TX, USA) with gold/palladium for 30 s. An accelerating voltage of 5–15 kV was used to view the images.

2.3.4. Dissolution testing at below equilibrium solubility

Dissolution testing at below equilibrium solubility was performed on the URF powder samples using a United States Pharmacopeia (USP) 27 Type 2 dissolution apparatus (VanKel VK6010 Dissolution Tester with a Vanderkamp VK650A heater/circulator, Varian, Inc. Palo Alto, CA). Powder samples (0.4 mg of TAC) equivalent to approximately 59% of the equilibrium solubility (6.8 μg/mL) were added to 100 mL of the modified simulated lung fluids (SLF) with 0.02% DPPC as dissolution media [29]. The dissolution media was maintained at 37.0 ± 0.2 °C and stirred at a constant rate of 50 rpm. Samples (1 mL) were withdrawn at 10, 20, 30, 60 and 120 min time points, filtered using a 0.45 μm GHP Acrodisc filter (VWR, Inc., West Chester, PA) and analyzed using a Shimadzu LC-10 liquid chromatograph (Shimadzu Corporation, Kyoto, Japan) equipped with an Alltech ODS-2, 5 μm C_{18} column (Alltech Associates, Inc., Deerfield, IL). The mobile phase consisted of a 70:30 (v/v) ACN:Water mixture, used at a flow rate of 1 mL/min. The maximum absorbance was measured at wavelength $\lambda_{max} = 214$ nm. These conditions gave well-resolved, sharp peaks for TAC with retention time of approximately 5.5 min. The limit of detection for TAC was 1 μg/mL and the limit of quantitation was of 2 μg/mL. System suitability requirements were met (correlation coefficient (R^2) $\geqslant$ 0.998, precision $\leqslant$ 2.0% RSD, theoretical plates > 500 plates/column and peak asymmetry < 1.5). A check standard was injected after each 5–10 unknown samples throughout the HPLC batch run.

2.3.5. Dissolution behavior in the formation of supersaturated solutions

Supersaturated dissolution profiles were generated according to the method described above (Section 2.3.4) except using the small volume dissolution apparatus equipped with a paddle stirring mechanism. Each drug formulation was weighed out which corresponded to approximately 15 times the aqueous crystalline solubility of TAC in 100 mL of the modified simulated lung fluid with 0.02% DPPC. Paddle speed and bath temperature were maintained at 100 rpm and 37 °C, respectively. An aliquot (1 mL) was removed from the small volume dissolution vessel at 10, 20, 30 and 60 min, then at 2, 4 and 24 h. Each aliquot was filtered through a 0.2 μm nylon filter, and a 0.5 mL aliquot of each filtered solution was immediately mixed with 1 mL of acetonitrile (to ensure no precipitation of drug previously dissolved at 37 °C). The samples were

analyzed for TAC concentration using the same HPLC procedure described above (Section 2.3.4). All experiments were performed in triplicate.

2.3.6. In vitro aerosol performance

The *in vitro* deposition characteristics of the dispersed and nebulized TAC formulations were investigated using a non-viable 8-stage cascade impactor (Thermo-Electron Corp., Symrna, GA, USA). The aerosolization behavior was described in terms of total emitted dose (TED), fine particle fractions (FPFs), mass median aerodynamic diameters (MMAD) and geometric standard deviation (GSD). The cascade impactor was assembled and operated in accordance with USP method 601 to assess the drug delivered. The powders were dispersed in water (10 mg/mL) and nebulized using an Aeroneb® Pro micropump nebulizer (Nektar Inc., San Carlos, CA) for 10 min at an air flow rate of 28.3 L/min. The flow rate was maintained by a vacuum pump (Emerson Electric Co., St. Louis, MO, USA) and calibrated by a TSI mass flow meter (Model 4000, TSI Inc., St. Paul, MN, USA). The mass deposited on each of the stages was collected and analyzed by HPLC as described in Section 2.3.4. Each experiment was repeated in triplicate.

2.4. In vivo mouse studies

2.4.1. Pulmonary administration of URF formulations

Pulmonary dosing of URF formulations was performed in healthy male ICR mice (Harlan Sprague Dawley, Inc., Indianapolis, IN). The study protocol was approved by the Institutional Animal Care and Use Committee (IACUCs) at the University of Texas at Austin, and all animals were maintained in accordance with the American Association for Accreditation of Laboratory Animal Care. Mice were acclimated and pre-conditioned in the restraint tube (Battelle, Inc., Columbus, OH) for 10–15 min/day for at least 2 days prior to dosing. Proper pre-conditioning is essential for reducing stress to mice, and maintaining a uniform respiration rate for the animals [32]. A small animal dosing apparatus for inhalation was used to dose the mice for this study. The dosing apparatus was designed to hold up to four mice as shown schematically in Fig. 2. The dosing apparatus consists of a small volume hollow tube with dimensions of 20×4.5 cm (nominal wall thickness of 0.4 cm) with four 1.75 cm adapter holes drilled at 7 cm intervals (two holes along each side). The adapter holes were constructed to accept rodent restraint tubes from the Battelle toxicology testing unit (Fig. 3).

The URF processed powders were re-dispersed in water (10 mg/mL) followed by sonication for 1 min prior to dosing. Nebulization of 3 mL of dispersions was conducted using an Aeroneb Pro ultrasonic nebulizer for 10 min dosing period. After pulmonary dosing, the mice were removed from the dosing apparatus and rested for 15 min. Two mice were sacrificed at each time point by CO_2 narcosis (0.5, 1, 2, 3, 6, 12, 24 and 48 h). Whole blood (1-mL aliquots) was obtained via cardiac puncture and analyzed according to the standard ELISA procedure as outlined in Section 2.4.2. In addition, necropsy was performed on each mouse to extract lung tissue. Samples were stored at −20 °C until assayed. TAC concentrations in lung tissue were determined using a previously HPLC assay as described in Section 2.3.4.

2.4.2. Enzyme-linked immunosorbent assay (ELISA) for analysis of TAC concentrations in blood

The determination of TAC in whole blood was performed using the PRO-Trac™ II FK 506 ELISA assay kit (Diasorin Inc., Stillwater, USA) in accordance with the manufacturer's instructions. Specifically, 50 μL of whole blood sample or standards was placed into a conical 1.5 mL polypropylene tube. Digestion reagent was freshly reconstituted, and 300 μL was added to all tubes. The tubes were vortexed for 30 s and incubated at room temperature for 15 min. These tubes were then placed on an aluminum heating block circulated with 75 °C water bath for 15 min to stop proteolysis. After vortexing, the tubes were centrifuged at room temperature at 1800*g* for 10 min. The supernatant (100 μL) was transferred to microtiter plate wells in duplicate from each centrifuged tube. Capture monoclonal anti-FK506 (50 μL) was added to each well, and the plate was shaken at room temperature at 700 rpm for 30 min. TAC horseradish peroxidase conjugate (50 μL) was then added to each well, and the plate was shaken at room temperature at 700 rpm for an additional 60 min. The plate was washed, before the addition of 200 μL chromogen. The plate was then shaken at 700 rpm for a further 15 min at room temperature. The subsequent reaction in each plate well was terminated by the addition of 100 μL of stop solution. The absorbance in each well was read at the dual wavelengths of 450 and 630 nm. Data were plotted

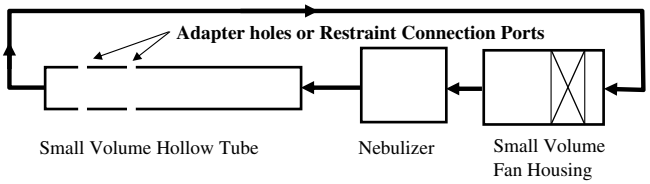

Fig. 2. Schematic diagram of small animal nose-only dosing apparatus.

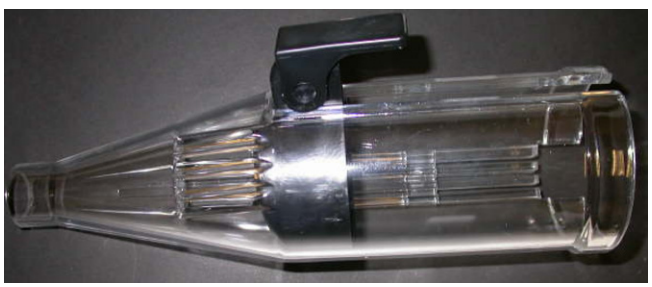

Fig. 3. Restraint tubes from the Battelle® toxicology testing unit.

according to a four-parameter logistic (4PL) curve-fitting program.

2.4.3. Solid phase extraction and drug analysis of lung tissues using HPLC

Lung extraction was carried out using solid phase extraction to obtain TAC levels using reverse phase HPLC. The total lung weight was recorded individually from each mouse. Lung tissues were homogenized using a Polytron rotor-stator homogenizer (VWR Scientific Corporation, West Chester, PA) for 40 s in 1 mL of normal saline. The homogenized lung samples were then mixed with 0.5 mL solution of 0.4 N zinc sulfate heptahydrate in the mixture of methanol/water (70:30) solution and vortex mixed for 30 s. Acetonitrile (1 mL) was added to the homogenized samples before a further vortex mixing for 1.5 min, followed by centrifugation at 3000 rpm for 15 min to obtain a clear supernatant. Next, the supernatant was collected into a clean vial containing 1 mL purified water. Meanwhile C18 cartridges for solid phase extraction (Supelco Inc., Bellefonte, PA) were pre-conditioned. First, these columns were pretreated with 2 mL of acetonitrile, followed by 1 mL methanol and then washed with 1 mL of water before loading the supernatant through the column. The sample was transferred and drawn slowly through the column by reducing the vacuum. The column was washed again by passing 1.5 mL mixture of methanol/water (70:30) solution, followed by 0.5 mL of *n*-hexane and allowed it to dry under vacuum. The sample was finally eluted with 2 mL of acetonitrile (0.5 mL × 4). The eluted material was evaporated under a dry nitrogen stream and then reconstituted with 250 μL of mobile phase using the previously described HPLC assay (Section 2.3.4). Data were expressed as μg TAC/gram wet lung tissue analyzed.

2.4.4. Pharmacokinetics and statistical analysis

The lung tissue concentration vs. time was investigated using a non-compartmental model, while the whole blood concentration vs. time was evaluated using one-compartmental analysis from extravascular administration (via the lung compartment). Pharmacokinetic parameters were calculated using WinNonlin version 4.1 (Pharsight Corporation, Mountain View, CA). The pharmacokinetic profile of TAC was characterized by maximum concentration (C_{max}), time to C_{max} (T_{max}), half-life ($T_{1/2}$) and area-under-the-curve (AUC) between 0 and 24 h. AUC was calculated using the trapezoidal rule; C_{max} and T_{max} were determined from the concentration-time profiles; $T_{1/2}$ was calculated by using the elimination rate constant (K_{el}); K_{el} was obtained from the ln concentration-time profiles.

The data sets were compared using a Student's *t*-test of the two samples assuming equal variances to evaluate the differences. The significance level ($\alpha = 0.05$) was based on the 95% probability value ($p < 0.05$).

3. Results and discussion

3.1. In vitro characterization of URF formulations

The physicochemical properties of TAC powders produced by URF were investigated and compared to the unprocessed TAC. The XRD patterns of the URF formulations and unprocessed TAC are shown in Fig. 4. The diffractogram of URF-TAC was similar to that of unprocessed TAC, indicating a high degree of crystallinity. However, the XRD pattern of URF-TAC:LAC confirmed that this composition was amorphous. This suggests that lactose inhibited crystallization of TAC. It is well known that sugars such as lactose can be used to stabilize amorphous drugs, peptides and proteins during drying and subsequent storage [33–35]. The addition of sugars has been shown to extend the shelf life of amorphous systems by preventing crystallization. In addition, lactose is generally regarded as safe (GRAS) for use as an excipient in inhalation systems [15]. This is due to its non-toxic and degradable properties after administration [36].

SEM micrographs of the two URF processed formulations are shown in Fig. 5. The micrographs show highly porous, nanostructured aggregates. The morphologies seen in the SEM of URF processed particles were composed of submicron primary particles with a diameter of approximately 100–200 nm. In contrast, the SEM micrograph of unprocessed TAC indicated an irregular, dense and large crystal plate measuring between 50 and 100 μm in size (Fig. 5c). Accordingly, the surface areas obtained by the URF processed formulations (URF-TAC:LAC and URF-TAC was 29.3 and 25.9 m^2/g, respectively) were significantly higher than ($p < 0.05$) that of the unprocessed drug (0.53 m^2/g). This result is in agreement with the porous nanostructured aggregates of the URF powders observed by SEM.

The *in vitro* aerosol performance measured by cascade impaction for aqueous dispersions prepared from the URF processed powders is presented in Table 1. Comparison of the data suggests similar aerodynamic properties of the drug particles aerosolized from the two URF formula-

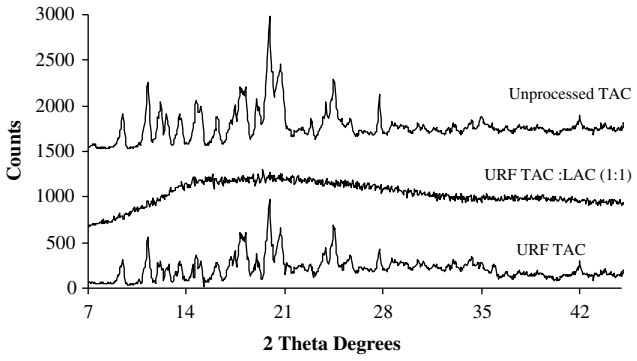

Fig. 4. X-ray diffraction profiles of TAC URF formulations compared to unprocessed TAC.

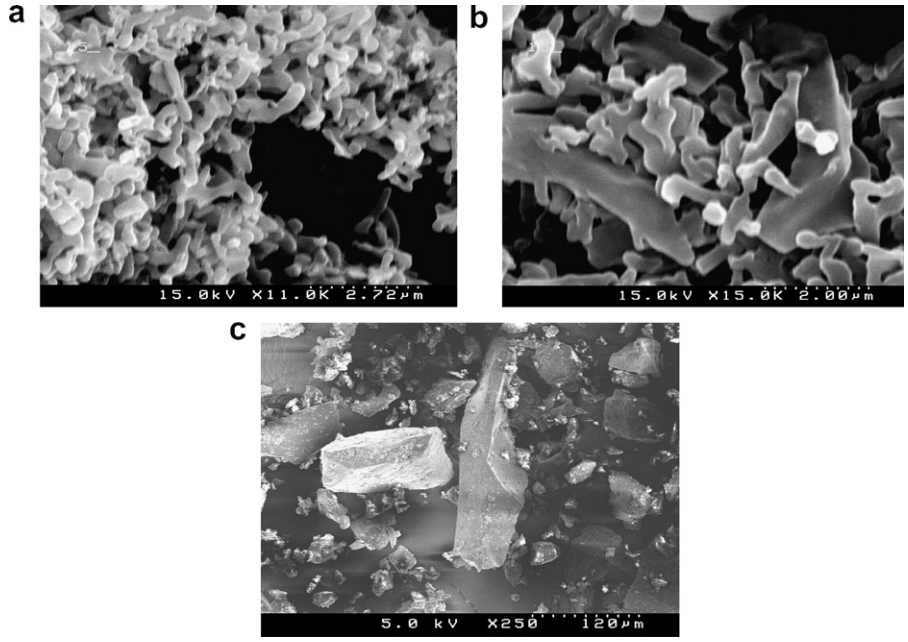

Fig. 5. SEM micrographs of (a) URF-TAC:LAC (1:1), (b) URF-TAC, (c) unprocessed TAC.

Table 1
Physicochemical properties of TAC powder compositions prepared by the URF process and aerosol characteristics of aqueous dispersions of URF powder compositions delivery by nebulization

Formulations	Physical state of drug	Surface area (m^2/g)	TED (μg)	%FPF	MMAD (μm)	GSD
URF-TAC:LAC	Amorphous	29.3	5082	74.6	2.57	2.24
URF-TAC	Crystalline	25.9	4823	70.2	2.86	1.97

TED, total emitted dose.
MMAD, mass median aerodynamic diameters.
GSD, geometric standard deviation.
FPF, fine particle fraction, as percentage of total loaded dose <5 μm.

tions. The MMAD was 2.57 and 2.86 μm for URF-TAC:LAC and URF-TAC, respectively, and the GSD was less than 2.2 (Table 1). It can be concluded that the aerosol droplets contain aggregates of nanoparticles that are in the respirable range by nebulization. Aerodynamic particle size is the most important parameter in determining drug deposition in the lungs and must be considered when developing formulations for pulmonary delivery [37]. Aerosolized particles or droplets with a MMAD ranging from 1 to 5 μm are suitable for deep lung deposition, at the site of the alveoli, where maximum absorption may take place [38]. The optimal aerosolization properties of both URF formulations are also reflected in the high %FPF ranging from 70% to 75%, illustrating efficient lung delivery of drug particles. The TED was only slightly higher for URF-TAC:LAC (5082 μg) compared to that of URF-TAC (4823 μg). These values were not significantly different ($p > 0.05$).

The *in vitro* dissolution profiles of TAC in SLF media under sink conditions are shown in Fig. 6. The dissolution rates for both URF processed powders were significantly increased ($p < 0.05$) as compared to the unprocessed TAC. Nanostructured aggregates of the URF processed powders were able to wet and dissolve quickly upon contact in SLF containing 0.02% DPPC, although the formulations contained no surfactant. For URF-TAC:LAC (i.e., amorphous, nanostructured aggregates), the dissolution of TAC was 72% in 30 min, compared to 67% for the URF-TAC (i.e., crystalline nanostructured aggregates) and 30% for the unprocessed TAC, respectively. The enhancement is most likely attributed to the high porosity and enhanced surface area of URF processed powders.

Dissolution of TAC at supersaturated conditions was also conducted in the same media. Supersaturated dissolution profiles of the URF processed formulations containing about 15 times the equilibrium solubility of TAC are compared in Fig. 7. The concentration obtained for the URF-TAC:LAC exceeded the equilibrium solubility of TAC, corresponding to a high degree of supersaturation in the SLF containing DPPC without the presence of surfactants or polymers in the formulation. The level of supersaturation corresponded to about 11 times the equilibrium solubility. This was due to the high-energy phase of the amorphous TAC particles. The maximum concentration

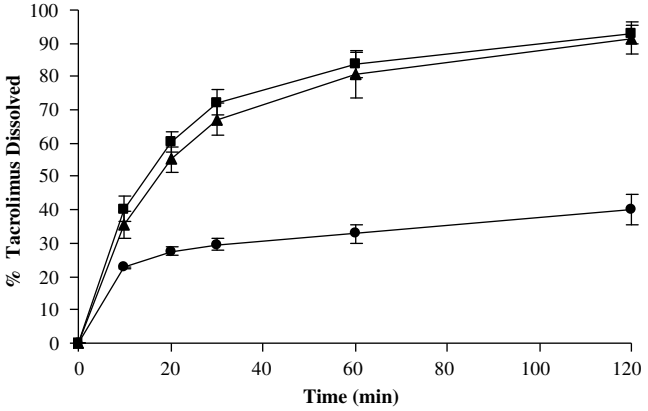

Fig. 6. Sink dissolution profiles for (■) amorphous URF composition TAC: lactose (1:1), (▲) crystalline URF composition TAC alone and (●) unprocessed TAC. The dissolution media were the modified simulated lung fluids (SLF) containing 0.02% DPPC at 100 rpm and 37 °C (equilibrium solubility of TAC in this medium ~6.8 μg/mL). Dissolution profiles were determined in replicates of 3.

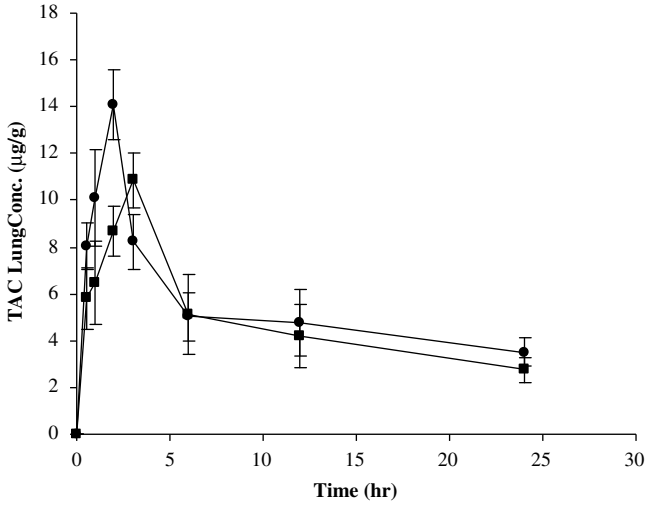

Fig. 8. Comparison of mean lung concentration (μg TAC/g tissue) vs. time profiles of the URF formulations. (●) Amorphous URF composition TAC: lactose (1:1) and (■) crystalline URF composition TAC alone.

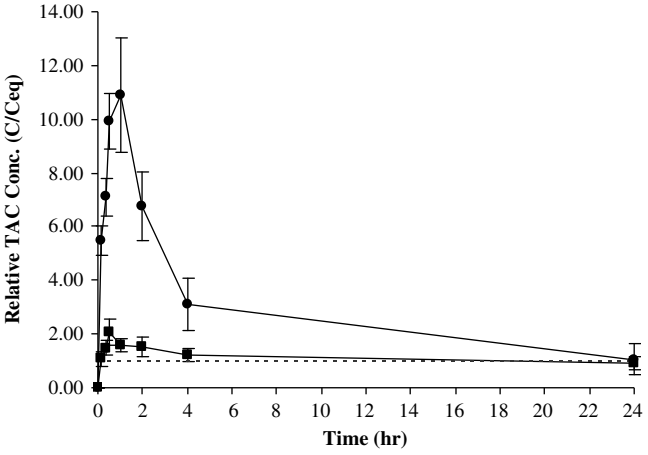

Fig. 7. Supersaturated dissolution profile for (●) amorphous URF composition TAC: lactose (1:1); (■) crystalline URF composition TAC alone and (---) equilibrium solubility of TAC in the dissolution media (6.8 μg/mL). The dissolution media were the modified simulated lung fluids (SLF) containing 0.02% DPPC at 100 rpm and 37 °C. Dissolution profiles were determined in replicates of 3.

occurred at 1 h, and then decreased to 3 times the equilibrium solubility over the next 4 h. A supersaturation dissolution profile was not observed for URF-TAC because of its crystalline nature.

3.2. In vivo pulmonary studies

The pharmacokinetic absorption studies were conducted in mice. The murine model has been very effective for small scale inhalation studies [32]. The lung tissue concentration-time profiles following a single inhalation dose are shown in Fig. 8 while the corresponding pharmacokinetic parameters summarized in Table 2. C_{max} for URF-TAC:LAC was significantly higher (14.09 μg/g) compared to URF-TAC (10.86 μg/g) whereas T_{max} was significantly lower ($p < 0.05$) for 2 h. This could perhaps as a result of a greater dissolved concentration, as seen in the vitro supersaturation results. However, no significant differences in AUC-values (0–24 h) were observed between the two URF formulations ($p > 0.05$). The results indicated that the amorphous nature of the particles affects the rate of drug absorption. TAC in the URF-TAC:LAC was eliminated according to a biphasic pattern with distribution phase and elimination phase. The similar elimination pattern was also found in the URF-TAC. The values of K_{el} were not significantly different between the two URF formulations ($p > 0.05$). The decreasing TAC concentration in the lung for both URF formulations is a consequence of drug distribution and transport into the systemic circulation, as well as particle elimination from the lung. It can be seen clearly that the shape of the biphasic lung concentration-time profile supports the transfer of nanostructured aggregates (either amorphous or crystalline) from the lung into the blood compartment. The measured levels

Table 2
In vivo pharmacokinetic parameters for the lung tissue concentrations of the URF formulations

Formulations	C_{max} (μg/g)	T_{max} (h)	K_{el} (h^{-1})	$T_{1/2}$ (h)	$AUC_{(0-24)}$ (μg h/g)
URF-TAC	10.86 ± 1.07	3	0.0346	20.02	111.19 ± 20.16
URF-TAC:LAC	14.09 ± 1.50	2	0.0334	20.75	122.42 ± 6.19

C_{max}, maximum concentration.
T_{max}, time to C_{max}.
K_{el}, elimination rate constant.
$T_{1/2}$, half-life.
$AUC_{(0-24)}$: area-under-the-curve between 0 and 24 h.

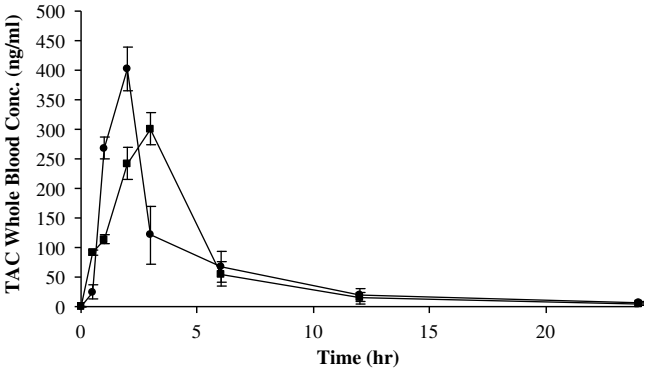

Fig. 9. Comparison of mean whole blood TAC concentration profiles of the URF formulations after a single inhalation administration. (●) Amorphous URF composition TAC: lactose (1:1) and (■) crystalline URF composition TAC alone.

for both URF formulations at 48 h were below the limit of quantification of the assay (determined to be 1 μg/g).

The systemic *in vivo* pharmacokinetic of drug absorption from the lungs was investigated in mice. Fig. 9 shows a comparison of mean whole blood concentration-time profiles from each formulation, and the calculated pharmacokinetic parameters following pulmonary administration are presented in Table 3. The whole blood concentration profile of each formulation has a similar absorption pattern, for example, T_{max}, compared to the lung concentration profiles (Fig. 8). However, both URF formulations demonstrated substantially lower TAC concentrations in the blood than was seen in the lung tissue. The whole blood profiles following pulmonary dosing of URF-TAC:LAC and URF-TAC had peak concentrations of 402.11 ng/mL at 2 h and 300.67 ng/mL at 3 h, respectively, before concentrations decreased. The $AUC_{(0–24)}$ (1235.66 ng h/mL) of the URF-TAC:LAC processed by URF is slightly lower than that of the URF-TAC (1324.35 ng h/mL), although there is no statistical difference ($p > 0.05$). The levels of TAC decreased rapidly for URF-TAC:LAC with the last time point with detectable levels occurring at 24 h, while URF-TAC declined in a similar but slower manner (no significant difference in the K_{el} values ($p > 0.05$)). Whole blood concentrations of TAC were below the limit of quantification for both formulations at 48 hours. The systemic and lung concentrations observed after nebulization of both URF formulations in mice suggest that a substantial lung and systemic exposure to TAC can be achieved in either amorphous nanostructured aggregates or crystalline nanostructured aggregates produced by URF. The observation that either amorphous or crystalline particles produced high systemic concentrations may suggest that high surface area was an important factor. High supersaturation, as a result of delivering amorphous particles in URF-TAC:LAC, correlated with faster absorption rates in both blood and lung tissue as compared to crystalline particles in URF-TAC. Use of supersaturated state in the lungs has not been previously studied yet. However, it has been demonstrated to enhance transdermal and oral absorption of poorly soluble drugs [39–41]. The *in vivo* data reported by Yamashita et al. [41] showed a high and extended systemic absorption of TAC following oral administration of amorphous solid dispersions with HPMC in beagle dogs. In the Yamashita et al. study, the solid dispersion of TAC with HPMC was prepared by solvent evaporation and was also shown to supersaturate in 0.1 N HCl up to 25 times in 2 h, and this level was maintained for over 24 h. The formation of a supersaturated state of amorphous particles may increase oral bioavailability of drug which suffer from poor/erratic bioavailability. In our study, supersaturation of TAC from URF-TAC:LAC showed no effect on the extent of drug absorption in both lung tissue and systemic circulation. This can be explained by the fact that supersaturation occurred over a short period of time for the absorption phase and then TAC concentration was rapidly decreased in the elimination phase.

4. Conclusions

High surface area, nanostructured aggregates containing amorphous or crystalline nanoparticles of TAC were produced by the URF process and shown to be effectively aerosolized in an aqueous dispersion by nebulization. Inclusion of lactose prevented crystallization of TAC and resulted in amorphous powder. URF-TAC:LAC (i.e., amorphous nanostructured aggregates) demonstrated the ability to supersaturate in SLF compared to the URF-TAC (i.e., crystalline nanostructured aggregates). Dispersions of nebulized URF formulations exhibited high lung and systemic concentrations. The $AUC_{(0–24)}$ of the URF formulations, which reflects the total amount of drug absorbed over the 24 h time period, was not significantly different ($p > 0.05$) for either lung or blood profiles. The

Table 3
In vivo pharmacokinetic parameters for the whole blood concentrations of the URF formulations following the pulmonary administration

Formulation	C_{max} (ng/mL)	T_{max} (h)	K_{el} (h^{-1})	$T_{1/2}$ (h)	$AUC_{(0–24)}$ (ng h/mL)
URF-TAC	300.67 ± 27.04	3	0.123	5.63	1324.35 ± 318.07
URF-TAC:LAC	402.11 ± 35.99	2	0.115	6.02	1235.66 ± 65.86

C_{max}, maximum concentration.
T_{max}, time to C_{max}.
K_{el}, elimination rate constant.
$T_{1/2}$, half-life.
$AUC_{(0–24)}$: area-under-the-curve between 0 and 24 h.

results indicate that high drug absorption in lung tissue and blood following pulmonary administration was primarily due to high surface area of nanostructured aggregates from both formulations. The ability to achieve high solubility in the lungs translated to high C_{max} values based on results of the *in vivo* studies. In addition, the absorption rate of the URF processed formulation containing amorphous TAC is faster than that of the formulation containing crystalline TAC. We have demonstrated that nanoparticles of TAC can be successfully delivered to the lungs without the use of polymers or surfactants.

Acknowledgment

The authors wish to gratefully acknowledge partial financial support from The Dow Chemical Company.

References

[1] M.A. Hooks, Tacrolimus, a new immunosuppressant – a review of the literature, Ann. Pharmacother. 28 (1994) 501–511.
[2] J.C. Waldrep, New aerosol drug delivery systems for the treatment of immune-mediated pulmonary diseases, Drugs Today 34 (1998) 549–561.
[3] K. Loser, S. Balkow, T. Higuchi, J. Apelt, A. Kuhn, T.A. Luger, S. Beissert, FK506 controls CD40L-induced systemic autoimmunity in mice, J. Invest. Dermatol. 126 (2006) 1307–1315.
[4] M.D. Tacca, Prospects for personalized immunosuppression: pharmacologic tools – review, Transplant. Proc. 36 (2004) 687–689.
[5] A.B. Jain, J.J. Fung, Cyclosporin and tacrolimus in clinical transplantation – a comparative review, Clin. Immunother. 5 (1996) 351–373.
[6] S. Tamura, Y. Tokunaga, R. Ibuki, G.L. Amidon, H. Sezaki, S. Yamashita, The site-specific transport and metabolism of tacrolimus in rat small intestine, J. Pharmacol. Exp. Ther. 306 (2003) 310–316.
[7] R. Venkataramanan, A. Swaminathan, T. Prasad, A. Jain, S. Zuckerman, V. Warty, J. McMichael, J. Lever, G. Burckart, T. Starzl, Clinical pharmacokinetics of tacrolimus, Clin. Pharmacokinet. 29 (1995) 404–430.
[8] R. Venkataramanan, L.M. Shaw, L. Sarkozi, R. Mullins, J. Pirsch, G. MacFarlane, D. Scheller, D. Ersfeld, M. Frick, W.E. Fitzsimmons, M. Virji, A. Jain, K.L. Brayman, A. Shaked, Clinical utility of monitoring tacrolimus blood concentrations in liver transplant patients, J. Clin. Pharmacol. 41 (2001) 542–551.
[9] Y. Kawashima, Nanoparticulate systems for improved drug delivery, Adv. Drug Deliv. Rev. 47 (2001) 1–2.
[10] A. Grenha, B. Seijo, C. Remunan-Lopez, Microencapsulated chitosan nanoparticles for lung protein delivery, Eur. J. Pharm. Sci. 25 (2005) 427–437.
[11] K.M.G. Taylor, O.N.M. McCallion, Ultrasonic nebulisers for pulmonary drug delivery, Int. J. Pharm. 153 (1997) 93–104.
[12] Y. Martinet, P. Pinkston, C. Saltini, J. Spurzem, J. Muller-Quernheim, R.G. Crystal, Evaluation of the in vitro and in vivo effects of cyclosporine on the lung T-lymphocyte alveolitis of active pulmonary sarcoidosis, Am. Rev. Respir. Dis. 138 (1988) 1242–1248.
[13] J.T. McConville, K.A. Overhoff, P. Sinswat, J.M. Vaughn, B.L. Frei, D.S. Burgess, R.L. Talbert, J.I. Peters, K.P. Johnston, R.O. Williams, Targeted high lung concentrations of itraconazole using nebulized dispersions in a murine model, Pharm. Res. 23 (2006) 901–911.
[14] I. Noboru, N. Takeshi, M. Keitarou, T. Tsutomu, T. Kenji, T. Tsunenori, S. Yorihisa, N. Mikiro, Efficacy and safety of inhaled Tacrolimus in rat lung transplantation, J.. Thorac. Cardiovasc. Surg. 2 (2007) 348–553.
[15] C. Bosquillon, C. Lombry, V. Preat, R. Vanbever, Influence of formulation excipients and physical characteristics of inhalation dry powders on their aerosolization performance, J. Control. Release 70 (2001) 329–339.
[16] S. Rossi, M.P. Buera, S. Moreno, J. Chirife, Stabilization of the restriction enzyme EcoRI dried with trehalose and other selected glass-forming solutes, Biotechnol. Prog. 13 (1997) 609–616.
[17] H. Steckel, F. Eskandar, K. Witthohn, The effect of formulation variables on the stability of nebulized aviscumine, Int. J. Pharm. 257 (2003) 181–194.
[18] J. Fu, J. Fiegel, E. Krauland, J. Hanes, New polymeric carriers for controlled drug delivery following inhalation or injection, Biomaterials 23 (2002) 4425–4433.
[19] G. Brambilla, D. Ganderton, R. Garzia, D. Lewis, B. Meakin, P. Ventura, Modulation of aerosol clouds produced by pressurised inhalation aerosols, Int. J. Pharm. 186 (1999) 53–61.
[20] R.J. Keenan, A. Zeevi, A.T. Iacono, K.J. Spichty, J.Z. Cai, S.A. Yousem, P. Ohori, I.L. Paradis, A. Kawai, B.P. Griffith, Efficacy of inhaled cyclosporine in lung transplant patients with refractory rejection: correlation of intragraft cytokine gene expression with pulmonary function and histologic characteristics, Surgery 118 (1995) 385–392.
[21] R.J. Keenan, A.J. Duncan, S.A. Yousem, M. Zenati, M. Schaper, R.D. Dowling, Y. Alarie, G.J. Burckart, B.P. Griffith, Improved immunosuppression with aerosolized cyclosporine in experimental pulmonary transplantation, Transplantation 53 (1992) 20–25.
[22] F. Blot, R. Tavakoli, S. Sellam, B. Epardeau, F. Faurisson, N. Bernard, M.-H. Becquemin, I. Frachon, M. Stern, J.-J. Pocidalo, C. Carbon, A. Bisson, I. Caubarrere, Nebulized cyclosporine for prevention of acute pulmonary allograft rejection in the rat: pharmacokinetic and histologic study, J. Heart Lung Transplant. 14 (1995) 1162–1172.
[23] J.C. Waldrep, J. Arppe, K.A. Jansa, M. Vidgren, Experimental pulmonary delivery of cyclosporin A by liposome aerosol, Int. J. Pharm. 160 (1998) 239–249.
[24] Z.S. Yu, T.L. Rogers, J.H. Hu, K.P. Johnston, R.O. Williams III, Preparation and characterization of microparticles containing peptide produced by a novel process: spray freezing into liquid, Eur. J. Pharm. Sci. 54 (2002) 221–228.
[25] T.L. Rogers, A.C. Nelsen, J.H. Hu, J.N. Brown, M. Sarkari, T.J. Young, K.P. Johnston, R.O. Williams III, A novel particle engineering technology to enhance dissolution of poorly water soluble drugs: spray-freezing into liquid, Eur. J. Pharm. Sci. 54 (2002) 271–280.
[26] T.L. Rogers, K.P. Johnston, R.O. Williams III, Solution-based particle formation of pharmaceutical powders by supercritical or compressed fluid CO2 and cryogenic spray-freezing technologies, Drug Dev. Ind. Pharm. 27 (2001) 1003–1015.
[27] T.L. Rogers, A.C. Nelsen, M. Sarkari, T.J. Young, K.P. Johnston, R.O. Williams III, Enhanced aqueous dissolution of a poorly water soluble drug by novel particle engineering technology: spray-freezing into liquid with atmospheric freeze-drying, Pharm. Res. 20 (2003) 485–493.
[28] T.L. Rogers, K.A. Overhoff, P. Shah, P. Santiago, M.J. Yacaman, K.P. Johnston, R.O. Williams III, Micronized powders of a poorly water soluble drug produced by a spray-freezing into liquid-emulsion process, Eur. J. Pharm. Sci. 55 (2003) 161–172.
[29] J.H. Hu, K.P. Johnston, R.O. Williams III, Stable amorphous danazol nanostructured powders with rapid dissolution rates produced by spray freezing into liquid, Drug Dev. Ind. Pharm. 30 (2004) 695–704.
[30] J.C. Evans, B.D. Scherzer, C.D. Tocco, G.B. Kupperblatt, J.N. Becker, D.L. Wilson, S. Saghir, E.J. Elder, Preparation of nanostructured particles of poorly water soluble drugs via a novel ultrarapid freezing technology, Polymeric Drug Delivery II: Polymeric Matrices and Drug Particle Engineering 924 (2006) 320–328.
[31] K.A. Overhoff, J.D. Engstrom, B. Chen, B.D. Scherzer, T.E. Milner, K.P. Johnston, R.O. Williams III, Novel ultra-rapid freezing particle

engineering process for enhancement of dissolution rates of poorly water-soluble drugs, Eur. J. Pharm. Sci. 65 (2007) 57–67.
[32] F.J. Miller, R.R. Mercer, J.D. Crapo, Lower respiratory-tract structure of laboratory-animals and humans – dosimetry implications, Aerosol. Sci. Tech. 18 (1993) 257–271.
[33] N.M. Davies, M.R. Feddah, A novel method for assessing dissolution of aerosol inhaler products, Int. J. Pharm. 255 (2003) 175–187.
[34] D.J.V. Drooge, W.L.J. Hinrichs, H.W. Frijlink, Incorporation of lipophilic drugs in sugar glasses by lyophilization using a mixture of water and tertiary butyl alcohol as solvent, J. Pharm. Sci. 93 (2004) 713–725.
[35] J.H.C. Eriksson, W.L.J. Hinrichs, G.J. de Jong, G.W. Somsen, H.W. Frijlink, Investigations into the stabilization of drugs by sugar glasses: III. The influence of various high-pH buffers, Pharm. Res. 20 (2003) 1437–1443.
[36] H. Wierik, P. Diepenmaat, Formulation of lactose for inhaled delivery systems, Pharm. Tech. Eur. 11 (2002) 1–5.
[37] A.H. de Boer, D. Gjaltema, P. Hagedoorn, H.W. Frijlink, Characterization of inhalation aerosols: a critical evaluation of cascade impactor analysis and laser diffraction technique, Int. J. Pharm. 249 (2002) 219–231.
[38] X.M. Zeng, G.P. Martin, C. Marriott, The controlled delivery of drugs to the lung, Int. J. Pharm. 124 (1995) 149–164.
[39] P. Gao, M.E. Guyton, T.H. Huang, J.M. Bauer, K.J. Stefanski, Q. Lu, Enhanced oral bioavailability of a poorly water soluble drug PNU-91325 by supersaturatable formulations, Drug Dev. Ind. Pharm. 30 (2004) 221–229.
[40] M. Iervolino, B. Cappello, S.L. Raghavan, J. Hadgraft, Penetration enhancement of ibuprofen from supersaturated solutions through human skin, Int. J. Pharm. 212 (2001) 131–141.
[41] K. Yamashita, T. Nakate, K. Okimoto, A. Ohike, Y. Tokunaga, R. Ibuki, K. Higaki, T. Kimura, Establishment of new preparation method for solid dispersion formulation of tacrolimus, Int. J. Pharm. 267 (2003) 79–91.